# A flight control design of a re-entry vehicle using a double-loop control system with fuzzy gain-scheduling

A Fujimori, P N Nikiforuk and M M Gupta

*Proceedings of the Institution of Mechanical Engineers, Part G: Journal of Aerospace Engineering* 2001 215: 1
DOI: 10.1243/0954410011531709

# A flight control design of a re-entry vehicle using a double-loop control system with fuzzy gain-scheduling

**A Fujimori**[1]*, **P N Nikiforuk**[2] and **M M Gupta**[2]
[1]Department of Mechanical Engineering, Shizuoka University, Hamamatsu, Japan
[2]Department of Mechanical Engineering, University of Saskatchewan, Saskatoon, Saskatchewan, Canada

**Abstract:** This paper presents a flight control design of an Automatic Landing FLight EXperiment (ALFLEX) vehicle using a double-loop control system (DLCS) with the fuzzy gain-scheduling (FGS) state feedback. The DLCS consists of an inner and an outer loop. The inner-loop control law is designed by the FGS state feedback to guarantee the stability over the entire operating range of the ALFLEX vehicle, while the outer loop control law is designed by a static gain to improve the tracking property. Futhermore, guidance laws for the longitudinal and the lateral directions are included in the control system to navigate the ALFLEX vehicle to a reference trajectory even if the initial condition is deviated from the nominal. The designed DLCS showed satisfactory performance in the numerical simulation of the ALFLEX vehicle.

**Keywords:** flight control, re-entry vehicle, gain-scheduling, double loop

## NOTATION

| | |
|---|---|
| $\mathbf{A}_i$, $\mathbf{B}_i$, $\mathbf{C}_i$, $\mathbf{D}_i$ | system matrices in the fuzzy model |
| $f(\boldsymbol{x}(t), \boldsymbol{u}(t))$ | non-linear state equation of the ALFLEX vehicle |
| $F_i$ | feedback gain |
| $g$ | gravity constant |
| $g(\boldsymbol{x}(t), \boldsymbol{u}(t))$ | non-linear state equation of the ALFLEX vehicle |
| $h_i$ | degree of satisfaction (grade) |
| $H$ | altitude |
| $K_{\text{in}}$ | inner-loop controller |
| $K_{\text{out}}$ | outer-loop controller |
| $K_1$ | feedforward controller of $K_{\text{in}}$ |
| $K_2$ | feedback controller of $K_{\text{in}}$ |
| $N_{ji}$ | fuzzy sets |
| $(p, q, r)$ | perturbed angular velocities from equilibrium values $(P_0, Q_0, R_0)$; $p \triangleq P - P_0$, $q \triangleq Q - Q_0$, $r \triangleq R - R_0$ |
| $(P, Q, R)$ | angular velocities with respect to the body axis |
| $s$ | Laplace transform variable |
| $t$ | time |
| $T_{zv}$ | transfer function from $z$ to $v$ |
| $T_{zz\text{c}}$ | transfer function from $z$ to $z_{\text{c}}$ |
| $(u, v, w)$ | perturbed velocities from equilibrium values $(U_0, V_0, W_0)$; $u \triangleq U - U_{\text{o}}$, $v \triangleq V - V_{\text{o}}$ and $w \triangleq W - W_0$ |
| $\boldsymbol{u}(t)$ | input vector |
| $(U, V, W)$ | velocities with respect to the body axis |
| $\boldsymbol{v}(t)$ | inner-loop command input vector |
| $V_{\text{air}}$ | flight velocity $= \sqrt{U^2 + V^2 + W^2}$ |
| $(V(t)$ | Lyapunov function |
| $\boldsymbol{x}(t)$ | state vector |
| $(x_{\text{e}}, y_{\text{e}}, z_{\text{e}})$ | Cartesian coordinate fixed at the runway |
| $\mathbf{X}$ | positive definite matrix |
| $(x_i^{\text{d}}, u_i^{\text{d}})$ | linearized point of $\dot{x} = f(\boldsymbol{x}(t), \boldsymbol{u}(t))$ |
| $\boldsymbol{z}(t)$ | controlled variable vector |
| $\boldsymbol{z}_{\text{c}}(t)$ | command vector of $\boldsymbol{z}(t)$ |
| $\alpha_i$ | normalized degree of satisfaction |
| $\gamma$ | perturbed flight path angle $= \theta - w/U_{\text{o}}$ |
| $\Gamma$ | flight path angle $= \Theta - W/U$ |
| $\delta_{\text{a}}, \delta_{\text{e}}, \delta_{\text{r}}, \delta_{\text{SB}}$ | deflection angles of aileron, elevator, rudder and speed brake |
| $(\Delta_{x\text{e}}, \Delta_{y\text{e}})$ | deviation of the release point |
| $\eta_j$ | variable which recognizes linearized points |
| $\mu_{ji}$ | membership function |
| $(\xi, y_{\text{e}}, \zeta)$ | Cartesian coordinate shifted by $x_{\text{off}}$ in the $x_{\text{e}}$ axis and rotated by $\theta_{\text{t}}$ from $(x_{\text{e}}, y_{\text{e}}, z_{\text{e}})$ |

*The MS was received on 29 September 1999 and was accepted after revision for publication on 19 October 2000.*
* *Corresponding author: Department of Mechanical Engineering, Shizuoka University, 3-5-1 Johoku, Hamamatsu 432-8561, Japan.*

| | |
|---|---|
| $(\omega, \theta, \psi)$ | perturbed Euler angles from equilibrium values $(\Phi_0, \Theta_0, \Psi_0)$; $\omega \triangleq \Phi - \Phi_0$, $\theta \triangleq \Theta - \Theta_0$ and $\psi \triangleq \Psi - \Psi_0$ |
| $(\Phi, \Theta, \Psi)$ | Euler angles |

**Acronyms**

| | |
|---|---|
| ALFLEX | Automatic Landing Flight Experiment |
| DLCS | double-loop control system |
| FGS | fuzzy gain-scheduling |
| LTI | linear time invariant |
| MDM/MDP | multiple delay models and multiple design points |
| NAL | National Aerospace Laboratory |
| NASDA | National Aerospace Development Agency |
| SLCS | single-loop control system |

## 1 INTRODUCTION

The National Aerospace Laboratory (NAL) and the National Aerospace Development Agency (NASDA) in Japan have been developing an unmanned re-entry space vehicle, named HOPE-X, for a decade [**1**]. Automatic Landing FLight EXperiment (ALFLEX) vehicle which is a 37 per cent sized model of the HOPE-X has been studied to develop an automatic landing control system [**2**–**4**]. Automatic landing flight tests of the ALFLEX vehicle were conducted at Woomera, Australia, in 1996 to evaluate aerodynamic characteristics and to develop flight control systems [**2, 4**]. Figure 1 is a simple diagram showing how the ALFLEX operates. The ALFLEX vehicle was dropped from a helicopter at an altitude of 1500 m with an initial velocity of 46 m/s and landed automatically on a runway. The ALFLEX vehicle had no thrusting equipment. The flight velocity was controlled by a speed brake, so the descending rate of the flight was high. Also, the characteristics of the ALFLEX vehicle was non-linear.

The NAL/NASDA designed a guidance and control law using a multiple delay models and multiple design points (MDM/MDP) approach [**2, 3**]. Other control techniques using inverse dynamics transformation [**5**] and neural networks [**6**] were proposed. To implement a reliable automatic control system on the HOPE-X, further studies of the flight control design of the ALFLEX vehicle are needed.

This paper presents an alternative flight control design for the ALFLEX vehicle using a double-loop control system (DLCS) with fuzzy gain-scheduling (FGS). The DLCS consists of an inner and an outer loop which are used to stabilize the controlled system and track the command respectively. In this paper, the inner-loop control law is determined by the FGS state feedback technique [**7**] to guarantee the stability over the entire operating range of the ALFLEX vehicle. The outer-loop control law is determined by static gain so as to improve the tracking property. Futhermore, guidance laws for the longitudinal and the lateral direction are included in the control system to navigate the ALFLEX vehicle to a reference trajectory even if the initial condition deviates from that required. The proposed control design method is applied to a numerical simulation program of the ALFLEX [**3**] to evaluate control performance of the designed control law.

## 2 AUTOMATIC LANDING FLIGHT EXPERIMENT

This section describes a re-entry vehicle used for ALFLEX. A sketch of the ALFLEX re-entry vehicle is shown in Fig. 2. The control surfaces are speed brake, rudder and elevon. The vehicle is geometrically similar to the HOPE-X built to a 37 per cent scale. The length and the span are 6.1 and 3.8 m respectively and the weight is 760 kg. Other physical parameters are given by the similarity rule in dynamics, which is associated with the reference length.

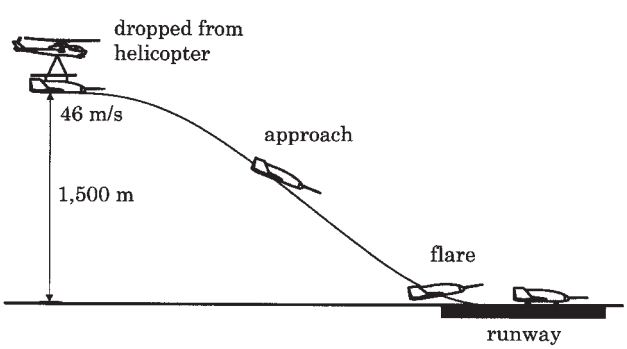


**Fig. 1** Automatic landing flight experiment

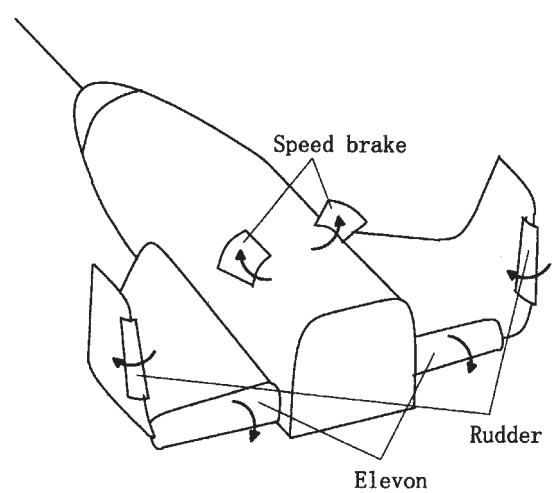


**Fig. 2** Sketch of the ALFLEX re-entry vehicle

The equation of motion of the ALFLEX vehicle is written as a non-linear equation:

$$\dot{\boldsymbol{x}}(t) = f(\boldsymbol{x}(t), \boldsymbol{u}(t))$$

$$\boldsymbol{z}(t) = g(\boldsymbol{x}(t), \boldsymbol{u}(t)) \tag{1}$$

where $\boldsymbol{x}(t)$ is the state vector given by

$$\boldsymbol{x}(t) = [U\,V\,W\,P\,Q\,R\,\Phi\,\Theta\,\Psi]^{\mathrm{T}} \tag{2}$$

where ($U$, $V$, $W$) and ($P$, $Q$, $R$) are respectively velocities and angular velocities with respect to the body axis and ($\Phi$, $\Theta$, $\Psi$) are Euler angles: $\boldsymbol{u}(t)$ is the input vector which consists of deflection angles of elevator $\delta_{\mathrm{e}}$, aileron $\delta_{\mathrm{a}}$, rudder $\delta_{\mathrm{r}}$ and speed brake $\delta_{\mathrm{SB}}$, given by

$$\boldsymbol{u}(t) = [\delta_{\mathrm{e}}\delta_{\alpha}\delta_{\mathrm{r}}\delta_{\mathrm{SB}}]^{\mathrm{T}} \tag{3}$$

where the deflection angle of the elevon is divided into the elevator angle $\delta_{\mathrm{e}}$ and the aileron angle $\delta_{\mathrm{a}}$ according to aerodynamic notation [**8**]. $\boldsymbol{z}(t)$ is the controlled variable vector whose elements are

$$\boldsymbol{z}(t) = [U\,\Gamma\,V\,\Phi]^{\mathrm{T}} \tag{4}$$

where $\Gamma$ is the flight path angle defined as $\Gamma \triangleq \Theta - W/U$.

In this paper, equation (1) is linearized at some equilibrium points to construct the fuzzy models in the FGS technique, which are presented in Section 4 of this paper. The equilibrium condition is that the dynamic pressure and the flight path angle are constant. The linearized equations are separated into the longitudinal and the lateral linear time-invariant (LTI) equations [**8**] whose state and input vectors are respectively given as:

Longitudinal LTI:

$$\boldsymbol{x}_{\mathrm{lon}} = [u\,w\,q\,\theta]^{\mathrm{T}}$$

$$\boldsymbol{u}_{\mathrm{lon}} = [\delta_{\mathrm{e}}\delta_{\mathrm{SB}}]^{\mathrm{T}}$$

$$\boldsymbol{z}_{\mathrm{lon}} = [\mu\gamma]^{\mathrm{T}} \tag{5}$$

Lateral LTI:

$$\boldsymbol{x}_{\mathrm{lat}} = [v\,p\,r\,\omega]^{\mathrm{T}}$$

$$\boldsymbol{u}_{\mathrm{lat}} = [\delta_{\mathrm{a}}\delta_{\mathrm{r}}]^{\mathrm{T}}$$

$$\boldsymbol{z}_{\mathrm{lat}} = [v\omega]^{\mathrm{T}} \tag{6}$$

The elements of the above vectors written in small letters indicate the difference of the elements written in large letters from the equilibrium value in equation (2); i.e. $u \triangleq U - U_0$, $\theta \triangleq \Theta - \Theta_0$, ..., where the subscript 0 means the value at the equilibrium point.

Table 1 shows eigenvalues of the longitudinal and lateral LTI models in which the altitude is $H = 1500, 600$ and 30 m. It is seen that the ALFLEX vehicle is unstable at almost the equilibrium points. Therefore, a control system is required to stabilize the ALFLEX vehicle on flight and to navigate it to a runway.

## 3 DOUBLE-LOOP CONTROL SYSTEM

Figure 3 shows a block diagram of a double-loop control system (DLCS) applying to a control design of the ALFLEX. $P$ is a controlled plant, $K_{\mathrm{in}}$ is an inner-loop controller and $K_{\mathrm{out}}$ is an outer-loop controller; $z$ is the controlled variable, $z_{\mathrm{c}}$ is its command input, $y$ is the feedback variable, $u$ is the control input and $v$ is the inner-loop command input. The ALFLEX vehicle is an unstable system and contains non-linear factors and uncertainties. The control system for the ALFLEX vehicle should therefore be designed not only to stabilize the controlled plant but also to compensate for tracking error $e \triangleq z_{\mathrm{c}} - z$ due to the non-linear factors and uncertainties. The inner loop is used for augmenting the stability of the system, while the outer loop is used for reinforcing the tracking property.

Use linear transfer functions to describe the outer loop of Fig. 3. Let $T_{zv}$ be the transfer function from $v$ to $z$. The transfer function from $z_{\mathrm{c}}$ to $z$, $T_{zz\mathrm{c}}$, is then written as

$$T_{zz\mathrm{c}} = (I + T_{zv}K_{\mathrm{out}})^{-1}T_{zv}(I + K_{\mathrm{out}}) \tag{7}$$

**Table 1** Eigenvalues of LTI models in which altitude is $H = 1500$ m

| Altitude (m) | Longitudinal | Lateral |
|---|---|---|
| 1500 | $-0.3115 \pm$ j0.1203 | $-1.7541 \pm$ j2.0076 |
| | $-4.8022, 0.1803$ | $0.6308, 0.3016$ |
| 600 | $-0.3519 \pm$ j0.0665 | $-1.8181 \pm$ j2.0192 |
| | $-4.9450, 0.1658$ | $0.6221, 0.3224$ |
| 30 | $-1.5206 \pm$ j0.5793 | $-1.3420 \pm$ j1.8875 |
| | $-0.0437 \pm$ j0.0821 | $0.2756 \pm$ j0.5679 |

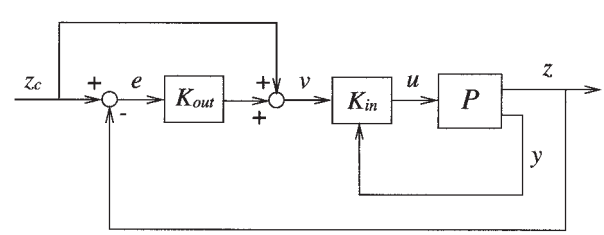


**Fig. 3** Double-loop control system

If $K_{in}$ is designed so as to stabilize the controlled plant and satisfy $T_{zv}(0) = I$, the steady state of $z$ for a step command $z_c$ is given by

$$z(\infty) = \lim_{s\to 0} sT_{zzc}(s)\frac{1}{s}z_c = z_c \tag{8}$$

The servo condition, equation (8), is always satisfied as long as $K_{out}$ stabilizes $T_{zv}$. Then, a guideline for designing the outer-loop controller $K_{out}$ is that $K_{out}$ is designed so as to stabilize $T_{zv}$ and improve the tracking property of $T_{zzc}$. The condition $T_{zv}(0) = I$ will be approximately satisfied by the inner-loop design, which is described in Section 4 below.

## 4 DESIGN OF THE INNER-LOOP CONTROLLER

The inner-loop controller $K_{in}$ is given by a two-degree-of-freedom controller:

$$K_{in} = [K_1 - K_2] \tag{9}$$

where $K_1$ is a feedforward controller to regulate the controlled variable $z(t)$ to the inner-loop command $v$ and $K_2$ is a feedback controller to stabilize the controlled plant. $K_{in}$ is designed by the fuzzy gain-scheduling (FGS) state feedback with non-zero set point input.

In this paper, the FGS technique for a linear parameter varying plant [7] is modified for the non-linear plant given by equation (1), where $\boldsymbol{x}(t) \in \mathscr{R}^n$ and $\boldsymbol{u}(t), \boldsymbol{z}(t) \in \mathscr{R}^m$. It is assumed that $\boldsymbol{x}(t)$ is available for feedback; i.e. $\boldsymbol{y}(t) = \boldsymbol{x}(t)$ in Fig. 3. When designing the inner loop, the outer loop is removed from Fig. 3. Then, the inner-loop command $v$ is equal to $z_c$.

### 4.1 Fuzzy model

Over the operating range of the system, select $r$ linearized points $(x_i^d, u_i^d)$ $(i = 1, \ldots, r)$ and construct an LTI model for each linearized point. Let $\eta_j (j = 1, \ldots, g)$ be variables which recognize the linearized points and $N_{ji} (i = 1, \ldots, r)$ be fuzzy sets of $\eta_j$. Fuzzy rules representing a non-linear system [equation (1)] is given as follows:

**If** $\eta_1 = N_{1i}$ and $\cdots$ and $\eta_g = N_{gi}$,
**Then** the non-linear system [equation (1)] is approximated by

$$\begin{bmatrix}\dot{\boldsymbol{x}}(t)\\ \boldsymbol{z}(t)\end{bmatrix} = \begin{bmatrix}\mathbf{A}_i & \mathbf{B}_i\\ \mathbf{C}_i & \mathbf{D}_i\end{bmatrix}\begin{bmatrix}\boldsymbol{x}(t) - x_i^d\\ \boldsymbol{u}(t) - u_i^d\end{bmatrix} + \begin{bmatrix}0\\ z^d\end{bmatrix} \qquad (i = 1, \ldots, r) \tag{10}$$

where

$$\mathbf{A}_i \triangleq \frac{\partial f(x_i^d, u_i^d)}{\partial x^T}, \qquad \mathbf{B}_i \triangleq \frac{\partial f(x_i^d, u_i^d)}{\partial u^T}$$

$$\mathbf{C}_i \triangleq \frac{\partial g(x_i^d, u_i^d)}{\partial x^T}, \qquad \mathbf{D}_i \triangleq \frac{\partial g(x_i^d, u_i^d)}{\partial u^T}$$

$N_{ji}$ is characterized by the membership function $\mu_{ji}(\eta_j)$. Figure 4 shows an example using the triangle membership function $\mu_{ji} \in [0, 1]$ for $N_{ji}$. When $\mu_{ji}$ is arranged in order of $i$, as shown in Fig. 4, a section between the $(i-1)$th and the $(i+1)$th points is interpolated by

$$\mu_{ji}(\eta_j) = \begin{cases} \dfrac{\eta_j - N_{ji-1}}{N_{ji} - N_{ji-1}} & (N_{ji-1} < \eta_j \leqslant N_{ji}) \\ \dfrac{\eta_j - N_{ji+1}}{N_{ji} - N_{ji+1}} & (N_{ji} < \eta_j \leqslant N_{ji+1}) \\ 0 & (\eta_j \leqslant N_{ji-1}, \eta_j > N_{ji+1}) \end{cases}$$
$$(j = 1, \ldots, g, \quad i = 1, \ldots, r) \tag{11}$$

To evaluate the suitability of a given set of $\eta_j (j = 1, \ldots, g)$, the degree of satisfaction $h_i(\eta)$ is given as

$$h_i(\eta) \triangleq \mu_{1i}(\eta_1) \wedge \cdots \wedge \mu_{gi}(\eta_g) \qquad (i = 1, \ldots, r) \tag{12}$$

where

$$\eta \triangleq [\eta_1 \cdots \eta_g]^T$$

and $\wedge$ is the minimum operator in fuzzy logic; i.e. the larger the value of $h_i(\eta)$, the more suitable is the $i$th LTI model [equation (10)] for the non-linear system of equation (1). Moreover, let $\alpha_i(\eta)$ be defined as the normalized degree of satisfaction:

$$\alpha_i(\eta) \triangleq \frac{h_i(\eta)}{\sum_{i=1}^{r} h_i(\eta)} \qquad (i = 1, \ldots, r) \tag{13}$$

where

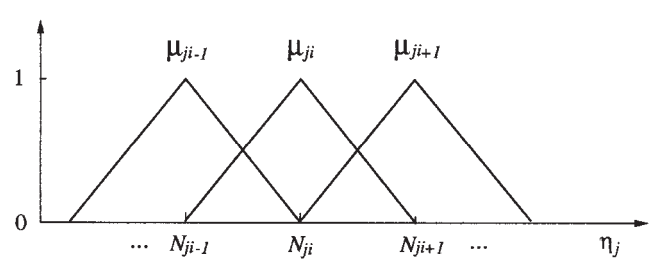


**Fig. 4** Fuzzy set using triangle membership functions

$$\alpha_i(\eta) \geqslant 0, \qquad \sum_{i=1}^{r} \alpha_i(\eta) = 1 \tag{14}$$

Thus, a model that corresponds to the entire operating range, i.e. a defuzzified model, is given by

$$\begin{bmatrix} \dot{\boldsymbol{x}}(t) \\ \boldsymbol{z}(t) \end{bmatrix} = \sum_{i=1}^{r} \alpha_i(\eta) \left( \begin{bmatrix} \mathbf{A}_i & \mathbf{B}_i \\ \mathbf{C}_i & \mathbf{D}_i \end{bmatrix} \begin{bmatrix} \boldsymbol{x}(t) - x_i^{\mathrm{d}} \\ \boldsymbol{u}(t) - u_i^{\mathrm{d}} \end{bmatrix} + \begin{bmatrix} 0 \\ z_i^{\mathrm{d}} \end{bmatrix} \right) \tag{15}$$

It is called the fuzzy model of the non-linear system [equation (1)].

### 4.2 Fuzzy gain-scheduling state feedback

Fuzzy rules of state feedback laws are given as follows:

**If** $\eta_1 = N_{1i}$ and $\cdots$ and $\eta_g = N_{gi}$,
**Then** a state feedback law is given by

$$\begin{aligned} \boldsymbol{u}(t) = &- F_i(\boldsymbol{x}(t) - x_i^{\mathrm{d}}) + u_i^{\mathrm{d}} \\ &+ K_1(v(\eta) - z_i^{\mathrm{d}}) \qquad (i = 1, \ldots, r) \end{aligned} \tag{16}$$

where $F_i (i = 1, \ldots, r)$ are $m \times n$ feedback gains and $v(\eta)$ is the feedforward input and is also the inner-loop command input of the DLCS. Equation (16) gives state feedback laws for $r$ linearized points. Similar to the fuzzy model, a state feedback law that corresponds to the entire operating range is given by

$$\boldsymbol{u}(t) = -\sum_{i=1}^{r} \alpha_i(\eta)[F_i(\boldsymbol{x}(t) - x_i^{\mathrm{d}}) - u_i^{\mathrm{d}} + K_1(v(\eta) - z_i^{\mathrm{d}})] \tag{17}$$

Equation (17) is called the fuzzy gain-scheduling (FGS) state feedback.

### 4.3 Design of feedback gain

Substituting equation (17) into equation (15), the closed inner-loop system is written as

$$\begin{aligned} \begin{bmatrix} \dot{\boldsymbol{x}}(t) \\ \boldsymbol{z}(t) \end{bmatrix} = &\begin{bmatrix} \tilde{\mathbf{A}}_{\mathrm{F}}(\eta) & \tilde{\mathbf{B}}(\eta)K_1 \\ \tilde{\mathbf{C}}_{\mathrm{F}}(\eta) & \tilde{\mathbf{D}}(\eta)K_1 \end{bmatrix} \begin{bmatrix} \boldsymbol{x}(t) \\ v(\eta) - \tilde{z}^{\mathrm{d}}(\eta) \end{bmatrix} \\ &+ \begin{bmatrix} w_1^{\mathrm{d}}(\eta) \\ w_2^{\mathrm{d}}(\eta) + z^{\mathrm{d}}(\eta) \end{bmatrix} \end{aligned} \tag{18}$$

where

$$\tilde{\mathbf{A}}_{\mathrm{F}}(\eta) \triangleq \sum_{i=1}^{r} \sum_{j=1}^{r} \alpha_i(\eta)\alpha_j(\eta)(\mathbf{A}_i - \mathbf{B}_i F_j)$$

$$\tilde{\mathbf{B}}(\eta) \triangleq \sum_{i=1}^{r} \alpha_i(\eta)\mathbf{B}_i$$

$$\tilde{\mathbf{C}}_{\mathrm{F}}(\eta) \triangleq \sum_{i=1}^{r} \sum_{j=1}^{r} \alpha_i(\eta)\alpha_j(\eta)(\mathbf{C}_i - \mathbf{D}_i F_j)$$

$$\tilde{\mathbf{D}}(\eta) \triangleq \sum_{i=1}^{r} \alpha_i(\eta)\mathbf{D}_i$$

$$\begin{aligned} w_1^{\mathrm{d}}(\eta) \triangleq &\sum_{i=1}^{r} \sum_{j=1}^{r} \alpha_i(\eta)\alpha_j(\eta) \\ &\times [\mathbf{B}_i(F_j x_j^{\mathrm{d}} + u_j^{\mathrm{d}}) - (\mathbf{A}_i x_i^{\mathrm{d}} + \mathbf{B}_i u_i^{\mathrm{d}})] \end{aligned}$$

$$\begin{aligned} w_2^{\mathrm{d}}(\eta) \triangleq &\sum_{i=1}^{r} \sum_{j=1}^{r} \alpha_i(\eta)\alpha_j(\eta) \\ &\times [\mathbf{D}_i(F_j x_j^{\mathrm{d}} + u_j^{\mathrm{d}}) - (\mathbf{C}_i x_i^{\mathrm{d}} + \mathbf{D}_i u_i^{\mathrm{d}})] \end{aligned}$$

$$\tilde{z}^{\mathrm{d}}(\eta) \triangleq \sum_{i=1}^{r} \alpha_i(\eta) z_i^{\mathrm{d}}$$

The feedback gains $F_i (i = 1, \ldots, r)$ are designed to guarantee the global stability over the entire operating range with the Lyapunov function. On the other hand, $K_1$ is designed to regulate $\boldsymbol{z}(t)$ to a step command $v = z_{\mathrm{c}}$.

The closed-loop system of equation (18) without external signals, i.e. $\dot{\boldsymbol{x}}(t) = \tilde{\mathbf{A}}_{\mathrm{F}}(\eta)\boldsymbol{x}(t)$, is quadratically stable only if there exists a Lyapunov function $V(t) \triangleq x^{\mathrm{T}}(t)\mathbf{X}^{-1}\boldsymbol{x}(t)$ such that

$$\dot{V}(t) \leqslant -\boldsymbol{x}^{\mathrm{T}}(t) \left[ \mathbf{Q} + \sum_{i=1}^{r} \alpha_i(\eta) F_i^{\mathrm{T}} \mathbf{R}_i F_i \right] \boldsymbol{x}(t) \tag{19}$$

where

$$\mathbf{Q} \geqslant 0, \qquad \mathbf{R}_i > 0 \qquad (i = 1, \ldots, r)$$

Since the external signals in equation (18), $w_1^{\mathrm{d}}(\eta)$, $w_2^{\mathrm{d}}(\eta)$, $\tilde{z}^{\mathrm{d}}(\eta)$ and $v(\eta)$, are bounded, the above stability condition is also held for equation (18) with external signals. For an LTI plant, i.e. $r = 1$ in equations (15) and (17), a sufficient condition where the linear quadratic regulator is quadratically stable is given by

$$\dot{\mathbf{V}}(t) \leqslant -\boldsymbol{x}^{\mathrm{T}}(t)\mathbf{Q}\boldsymbol{x}(t) - \boldsymbol{u}^{\mathrm{T}}(t)\mathbf{R}_1\boldsymbol{u}(t) \tag{20}$$

Equation (19) with $r > 1$ is obtained by extending equation (20) to the fuzzy model of equation (15) with the FGS state feedback equation (17).

Feedback gains $F_i (i = 1, \ldots, r)$ which satisfy the above

quadratic stability condition are parameterized by linear matrix inequalities (LMIs) [**9**] in the following theorem [**7**].

*Theorem 1*

Equation (19) is held only if there exist a positive-definite matrix $\mathbf{X}$ and matrices $\mathbf{M}_i (i = 1, \ldots, r)$ such that

$$\begin{bmatrix} \mathbf{A}_i\mathbf{X} + \mathbf{X}\mathbf{A}_i^{\mathrm{T}} - \mathbf{B}_i\mathbf{M}_i - \mathbf{M}_i^{\mathrm{T}}\mathbf{B}_i^{\mathrm{T}} & \mathbf{X}\mathbf{L}^{\mathrm{T}} & \mathbf{M}_i^{\mathrm{T}} \\ \mathbf{L}\mathbf{X} & -I_p & 0 \\ \mathbf{M}_i & 0 & -\mathbf{R}_i^{-1} \end{bmatrix} \leqslant 0 \qquad (i = 1, \ldots, r) \tag{21}$$

$$\begin{bmatrix} (\mathbf{A}_i + \mathbf{A}_j)\mathbf{X} + \mathbf{X}(\mathbf{A}_i + \mathbf{A}_j)^{\mathrm{T}} & \mathbf{X}\mathbf{H}^{\mathrm{T}} \\ -(\mathbf{B}_i\mathbf{M}_j + \mathbf{B}_j\mathbf{M}_i) - (\mathbf{B}_i\mathbf{M}_j + \mathbf{B}_j\mathbf{M}_i)^{\mathrm{T}} & \\ \mathbf{H}\mathbf{X} & -\frac{1}{2}I_p \end{bmatrix} \leqslant 0 \qquad (i = 1, \ldots, r, \quad j = i + 1, \ldots, r) \tag{22}$$

where $\mathbf{Q} = \mathbf{L}^{\mathrm{T}}\mathbf{L}$ and rank $\mathbf{Q} = p$. Then $F_i (i = 1, \ldots, r)$ in equation (17) are given by

$$F_i = \mathbf{M}_i\mathbf{X}^{-1} \qquad (i = 1, \ldots, r) \tag{23}$$

The proof is given in the Appendix.

### 4.4 Design of the feedforward controller

From equation (18), the steady states of $\boldsymbol{x}(t)$ and $\boldsymbol{z}(t)$ are obtained as

$$\boldsymbol{x}(\infty) = -\tilde{\mathbf{A}}_{\mathrm{F}}^{-1}[w_1^{\mathrm{d}} + \tilde{\mathbf{B}}K_1(v(\eta) - \tilde{z}^{\mathrm{d}}(\eta))] \tag{24}$$

$$\boldsymbol{z}(\infty) = \tilde{\mathbf{C}}_{\mathrm{F}}\boldsymbol{x}(\infty) + \tilde{\mathbf{D}}K_1(v(\eta) - \tilde{z}^{\mathrm{d}}(\eta)) + w_2^{\mathrm{d}} + \tilde{z}^{\mathrm{d}} \tag{25}$$

If $\tilde{\mathbf{D}} - \tilde{\mathbf{C}}_{\mathrm{F}}\tilde{\mathbf{A}}_{\mathrm{F}}^{-1}\tilde{\mathbf{B}}$ is invertible, then

$$K_1(v(\eta) - \tilde{z}^{\mathrm{d}}(\eta)) = (\tilde{\mathbf{D}} - \tilde{\mathbf{C}}_{\mathrm{F}}\tilde{\mathbf{A}}_{\mathrm{F}}^{-1}\tilde{\mathbf{B}})^{-1} \times (z_{\mathrm{c}} - \tilde{z}^{\mathrm{d}} + \tilde{\mathbf{C}}_{\mathrm{F}}\tilde{\mathbf{A}}_{\mathrm{F}}^{-1}w_1^{\mathrm{d}} - w_2^{\mathrm{d}}) \tag{26}$$

In equation (26), the term $\tilde{\mathbf{C}}_{\mathrm{F}}\tilde{\mathbf{A}}_{\mathrm{F}}^{-1}w_1^{\mathrm{d}} - w_2^{\mathrm{d}}$ is an error due to interpolation of the original non-linear plant among linearized points. If the linearized points $(\boldsymbol{x}^{\mathrm{d}}(t), \boldsymbol{u}^{\mathrm{d}}(t))$ can be continuously used over the entire operating range, $\tilde{\mathbf{C}}_{\mathrm{F}}\tilde{\mathbf{A}}_{\mathrm{F}}^{-1}w_1^{\mathrm{d}} - w_2^{\mathrm{d}}$ is zero. This term is neglected for the design of $K_1$. In the inner-loop design, the outer loop is removed; i.e. $v = z_{\mathrm{c}}$. Using these in equation (26), $K_1$ is given by

$$K_1 = (\tilde{\mathbf{D}} - \tilde{\mathbf{C}}_{\mathrm{F}}\tilde{\mathbf{A}}_{\mathrm{F}}^{-}\tilde{\mathbf{B}})^{-1} \tag{27}$$

Finally, the inner-loop controller $K_{\mathrm{in}}$ is given by

$$K_{\mathrm{in}} = [K_1 - K_2] = \left[(\tilde{\mathbf{D}} - \tilde{\mathbf{C}}_{\mathrm{F}}\tilde{\mathbf{A}}_{\mathrm{F}}^{-1}\tilde{\mathbf{B}})^{-1} - \sum_{i=1}^{r}\alpha_i(\eta)F_i\right] \tag{28}$$

From the above discussion, the condition $T_{zv}(0) = I$ is approximately satisfied by using $K_{\mathrm{in}}$ given by equation (28).

To summarize this section, a design procedure of the proposed DLCS with the FGS state feedback is given as follows:

*Step 1*. Define the variables $\eta_j (j = 1, \ldots, g)$ which recognize the linearized points.
*Step 2*. Choose $r$ linearized points (equilibrium points) and construct an LTI model $(\mathbf{A}_i, \mathbf{B}_i, \mathbf{C}_i, \mathbf{D}_i)$ at each linearized point.
*Step 3*. Construct a fuzzy model [equation (15)]; i.e. define the membership function $\mu_{ji}(\eta)$ and obtain the normalized degree of satisfaction $\alpha_i(\eta)$.
*Step 4*. Obtain $F_i (i = 1, \ldots, r)$ from equation (23); i.e. select weights $Q$ and $R_i (i = 1, \ldots, r)$ in the derivative of the Lyapunov function $V$ in equation (19) and find $\mathbf{X} > 0$ and $\mathbf{M}_i$ $(i = 1, \ldots, r)$ satisfying equations (21) and (22).
*Step 5*. Calculate $K_1$ from equation (27). Construct $K_{\mathrm{in}}$ from equation (28).
*Step 6*. Design $K_{\mathrm{out}}$ to stabilize $T_{zv}$ and to improve the tracking property of $T_{zz\mathrm{c}}$.

In step 6, $T_{zv}$ may be approximated by a low-order linear model $P_{\mathrm{m}}$ for designing $K_{\mathrm{out}}$. Since LTI models and gains for the FGS state feedback are obtained in steps 2 and 4, $P_m$ may be given by using them.

## 5 DESIGN OF GUIDANCE LAW

Generally speaking, re-entry space vehicles may deviate from a reference trajectory in practice. Should a deviation occur, the re-entry vehicle must be navigated to the reference trajectory and land on a runway. In the automatic landing flight test, the ALFLEX re-entry vehicle is released from a helicopter at an altitude of 1500 m, with the initial velocity of 46 m/s, as shown in Fig. 1 [**3**]. Then, a guidance law is needed to navigate the ALFLEX vehicle to the touchdown point, even if the release point deviates from the nominal release point. In this paper, a guidance law for the longitudinal direction is given by the reference flight path angle $\Gamma^*$ to catch up with the longitudinal reference

   

trajectory. On the other hand, a guidance law for the lateral direction is given by the reference roll angle $\Phi^*$ to modify the lateral deviation.

### 5.1 *Longitudinal direction*

Figure 5 shows a longitudinal reference trajectory whose original point is on a runway. Let $(x_e, y_e, z_e)$ be the Cartesian coordinate fixed at the runway, where the positive $y_e$ axis is upward. Introducing another coordinate $(\xi, y_e, \zeta)$, which is shifted by $x_{off}$ in the $x_e$ axis and is rotated by $\theta_t$ from $(x_e, y_e, z_e)$, the reference trajectory is given by the negative $\xi$ axis. $\theta_t$ is a slope angle of the longitudinal reference trajectory.

The relation between the flight path angle $\Gamma$ and $\zeta$ is given by

$$\frac{\dot{\zeta}}{V_{air}} = -\sin(\Gamma - \theta_t) \simeq -(\Gamma - \theta_t) \tag{29}$$

for small values of $|\Gamma - \theta_t|$. Using the Laplace transform,

$$\frac{\zeta(s)}{\Gamma(s) - \theta_t} = -\frac{V_{air}}{s} \tag{30}$$

Then $\zeta$ can be stabilized and tracked to a step command $\zeta_c$ by a proportional feedback:

$$\Gamma = K_t(\zeta - \zeta_c) + \theta_t \qquad (K_t > 0) \tag{31}$$

As shown in Fig. 5, the reference trajectory is given by the negative $\xi$ axis. Then $\zeta_c$ is given by $\zeta_c = 0$. Finally, the reference flight path angle of the ALFLEX vehicle is given by

$$\Gamma^* = K_t\zeta + \theta_t \tag{32}$$

where

$$\zeta = (x_e + x_{off})\sin\theta_t + z_e\cos\theta_t \tag{33}$$

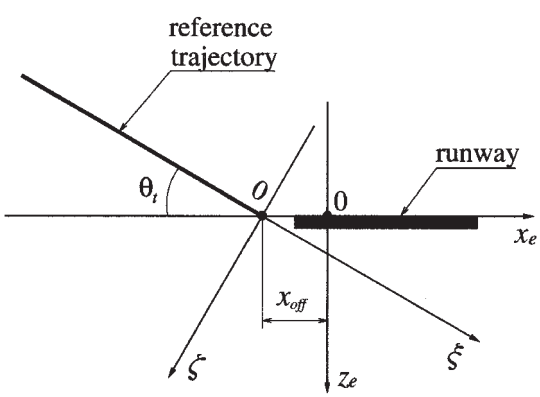


**Fig. 5** Longitudinal guidance law

### 5.2 *Lateral direction*

Supposing that the lateral motion is excited by only the roll motion, the equation of motion in the $y_e$ axis is given by

$$\ddot{y}_e = g\cos\Theta_0\Phi \tag{34}$$

where $g$ is the gravity constant. Using the Laplace transform in equation (34), a transfer function from $\Phi$ to $y_e$ is given by

$$\frac{y_e(s)}{\Phi(s)} = \frac{g\cos\Theta_0}{s^2} \tag{35}$$

Here $y_e$ is stabilized and is tracked to a step command $y_c$ by a feedback of $y_e$ and $\dot{y}$. The reference roll angle $\Phi^*$ is then given by

$$\Phi^* = -K_y(y_e - y_c) - K_{\dot{y}}\dot{y}_e \tag{36}$$

where $K_y$ and $K_{\dot{y}}$ are positive gains.

## 6 NUMERICAL SIMULATION OF ALFLEX

### 6.1 *Design of DLCS*

This section presents a numerical simulation in which the proposed control design method was applied to the ALFLEX flight control problem. The longitudinal reference trajectory was given with respect to the altitude $H$, as shown in Table 2. Since the ALFLEX vehicle has no thrusting equipment, the equation of motion of the ALFLEX vehicle depends on the altitude $H$. Then $\eta$ for constructing the fuzzy model was given by

$$\eta = \eta_1 = H \tag{37}$$

The non-linear equation of the ALFLEX vehicle [equation (1)] was linearized at the six equilibrium points shown in Table 3. At each equilibrium point, a linearized equation was separated into the longitudinal and the lateral LTI equations. The membership function of $H$,

$$\mu_H(H) = h_1(H) = \alpha_1(H) \tag{38}$$

was given as Fig. 6. Using the degree of satisfaction, fuzzy models were constructed for the longitudinal and the lateral directions respectively.

**Table 2** Reference flight velocity and reference flight path angle of the ALFLEX

| | $H \geqslant 90$ | $90 > H \geqslant 20$ | $20 > H$ |
|---|---|---|---|
| $V_{air}$(m/s) | 80 | 55 | 50 |
| $\Gamma$(deg) | −30 | −20 | −2 |

**Table 3** Linearized points with respect to flight velocity and flight path angle

| | Model 1 | Model 2 | Model 3 | Model 4 | Model 5 | Model 6 |
|---|---|---|---|---|---|---|
| $H$(m) | 1500 | 1000 | 600 | 100 | 30 | 1 |
| $V_{air}$(m/s) | 80 | 80 | 80 | 80 | 60 | 55 |
| $\Gamma$(deg) | −30 | −30 | −30 | −20 | −15 | −13 |

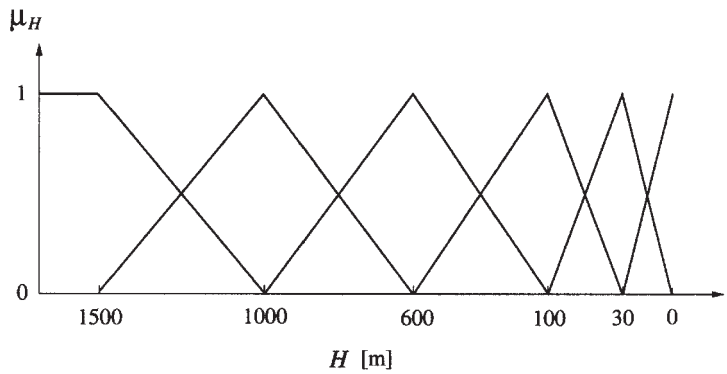


**Fig. 6** Membership function of $H$

The weighting matrices $\mathbf{Q}$ and $\mathbf{R}_i$ in equation (19) were given by

$$\mathbf{Q} = 0, \qquad \mathbf{R}_i = 125I_2 \qquad (i = 1, \ldots, 6) \tag{39}$$

MATLAB and the LMI Control Toolbox [**10**] were used to find a positive-definite matrix $\mathbf{X}$ and matrices $\mathbf{M}_i(i = 1, \ldots, 6)$ satisfying equations (21) and (22) and to obtain the state feedback gains $F_i(i = 1, \ldots, 6)$ in equation (23).

The inner-loop linear transfer function $T_{zv}$ at $H =$ 600 m was used to design $K_{\text{out}}$. In this simulation, the outer-loop controllers for the longitudinal and the lateral directions were obtained by static gains to stabilize $T_{zv}$ and to improve the tracking property of $T_{zz_c}$. Figure 7 shows the step responses of the perturbed velocity component along the $x$ axis, $u \triangleq U - U_0$, and the perturbed flight path angle, $\gamma \triangleq \Gamma - \Gamma_0$, where the designed $K_{\text{out}}$ was applied to $T_{zv}$ at $H = 600$ m and the command input was given by $z_c = [u^* \quad \gamma^*]^T = [20 \quad -10 \times \pi/180]^T$. Similarly, Fig. 8 shows the step responses of the perturbed velocity component along the $y$ axis, $v \triangleq V - V_0$, and the perturbed roll angle, $\omega \triangleq \Phi - \Phi_0$, where the command input was given by $z_c = [v^* \quad \omega^*]^T = [2 \quad 1 \times \pi/180]^T$. The solid lines show the responses of the DLCS, while the dashed lines show the responses of the single-loop control system (SLCS) in which the outer loop was removed from the DLCS and $v = z_c$. Comparing the solid lines to the dashed lines, the designed $K_{\text{out}}$ improved the settling property of the controlled variables.

Figures 9 and 10 show the initial time responses of the longitudinal and lateral guidance, where the guidance laws, equations (32) and (36), were substituted into equations (29) and (34) respectively. The feedback gains in equations (32) and (36) were given by $K_t = 0.1$, $K_y = 0.02828$ and $K_{\dot{y}} = 0.1621$. The slope angle $\theta_t$ was given by $\theta_t = -30°$. The solid lines show the responses with limiters of $-60 \leqslant \Gamma^* \leqslant 10°$ and $-35 \leqslant \Phi^* \leqslant 35°$ by taking into

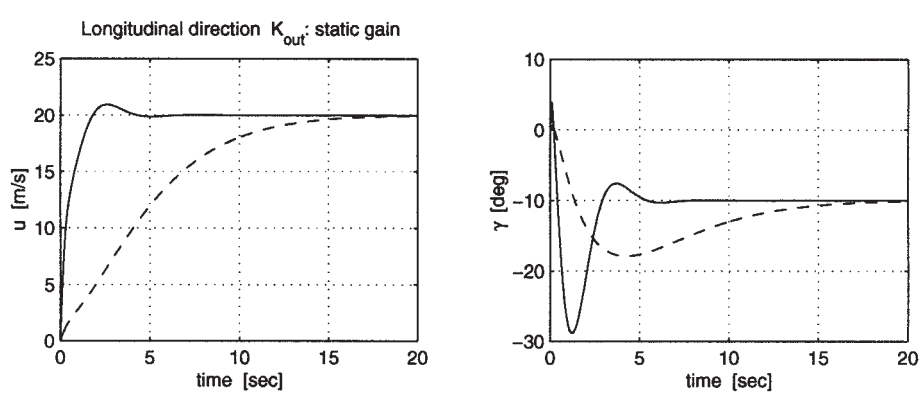


**Fig. 7** Step responses of the DLCS (solid line) and the SLCS (dashed line) for $z_c = [20 \quad -10 \times \pi/180]^T$

  

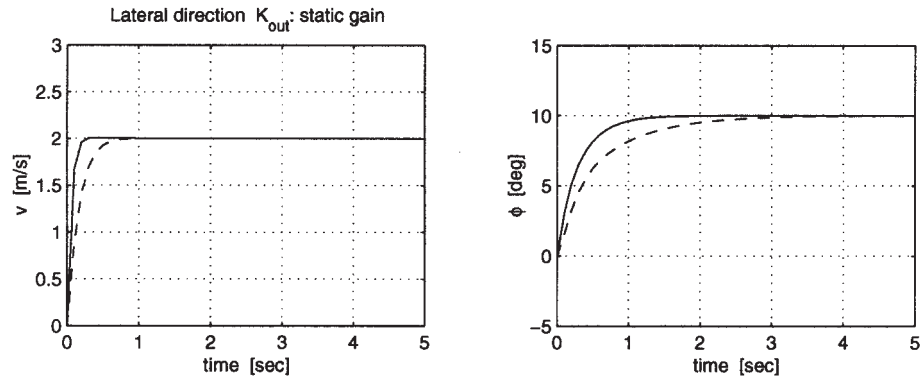


**Fig. 8** Step responses of the DLCS (solid line) and the SLCS (dashed line) for $z_c = [2 \quad 1 \times \pi/180]^T$

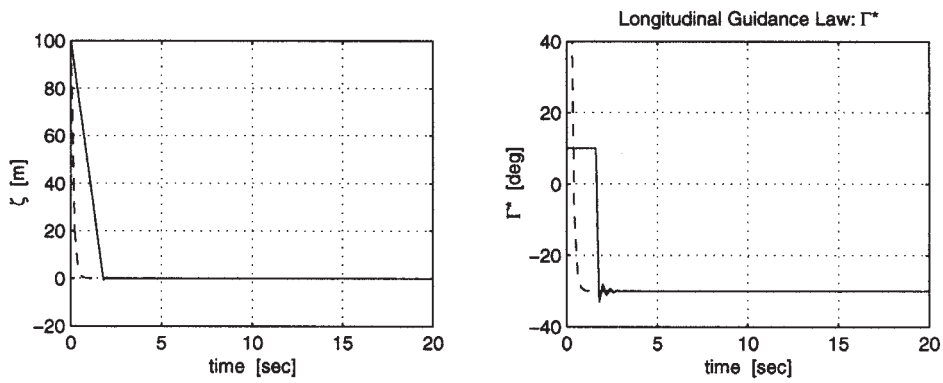


**Fig. 9** Initial time responses of $\zeta$ and $\Gamma^*$, where the initial offset of $\zeta$ is given by $\zeta(0) = 100$ m (solid line, with limiter; dashed line, without limiter)

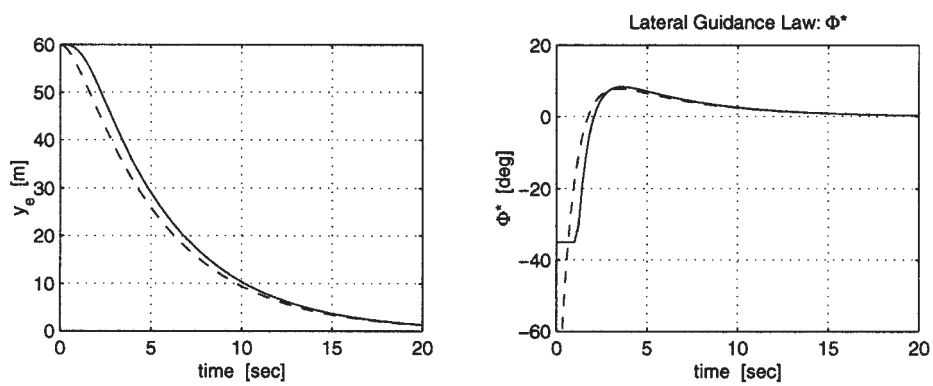


**Fig. 10** Initial time responses of $y_e$ and $\Phi^*$, where the initial offset of $y_e$ is given by $y_e(0) = 60$ m (solid line, with limiter; dashed line, without limiter)

account the operating ranges of the control surfaces, while the dashed lines show the responses without the limiters. Even if the limiters were included in the control systems, $\zeta$ and $y_e$ were settled to their references. Comparing both figures, it can be seen that the lateral guidance was slower than the longitudinal guidance to avoid lateral instability.

### 6.2 *Simulation results*

The designed DLCS was evaluated by a simulation program of the ALFLEX. The program included several components of the ALFLEX: aerodynamic models, actuators, atmospheric conditions, measurement systems, etc, [**3**].

Figures 11 to 14 show the time responses of the controlled variables and the control surfaces by the DLCS and the SLCS respectively. As given in Table 2, the reference flight velocity and the reference flight path angle for $H > 90$ m were given as $V_{air} = 80$ m/s and $\Gamma = -30°$. The tracking property of the DLCS was better than that of

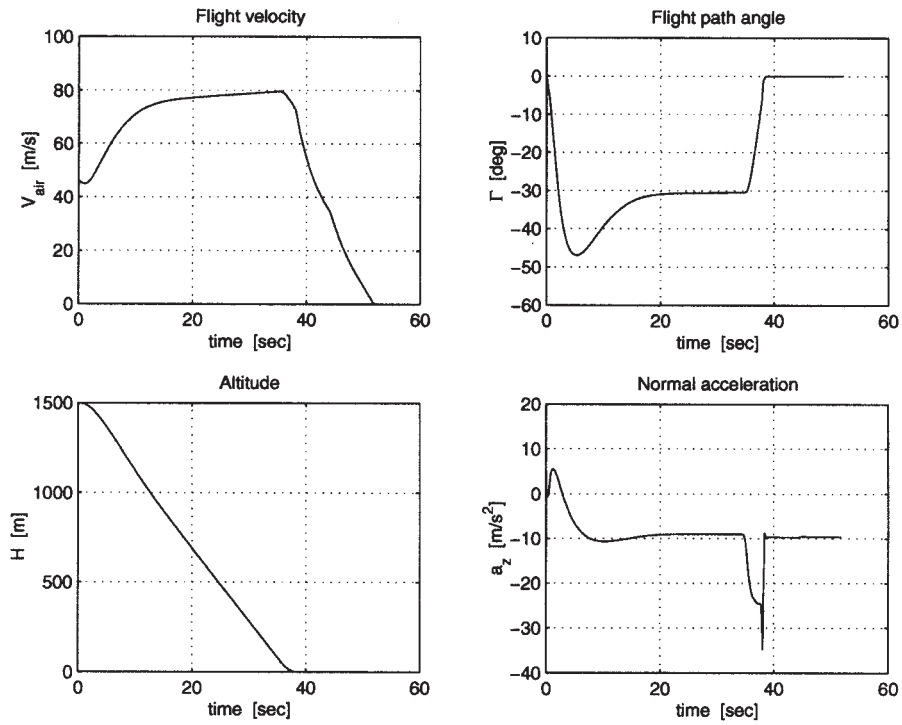


**Fig. 11** Time responses of controlled variables from release to landing by the SLCS

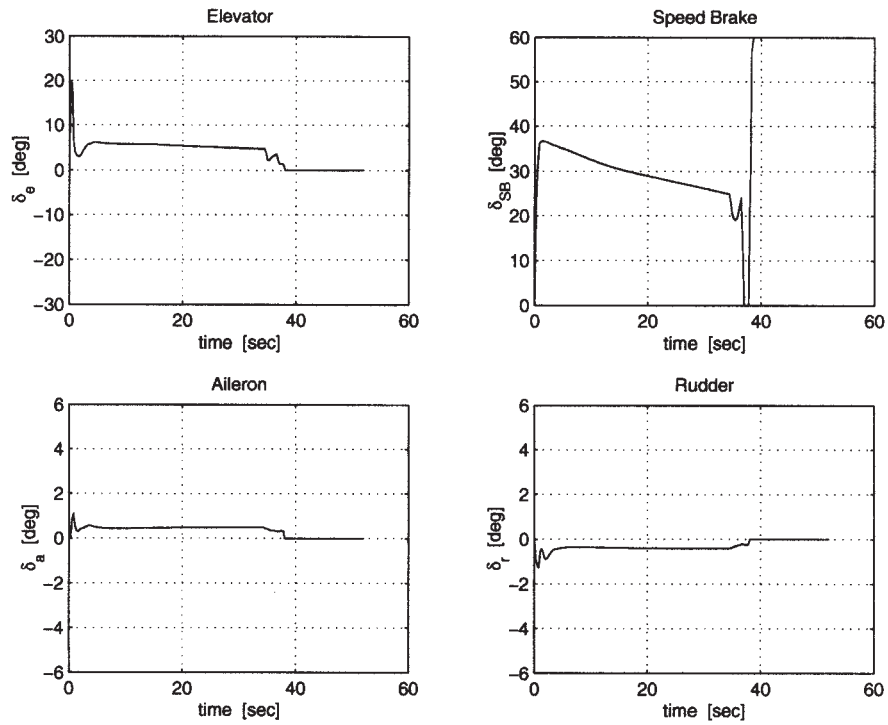


**Fig. 12** Time responses of control surfaces by the SLCS

the SLCS. This result from the activity of the elevator and the speed brake during the first 10 can be seen by comparing Fig. 12 with Fig. 14. The outer-loop controller $K_{out}$ provided a complementary input to reduce the tracking errors of $V_{air}$ and $\Gamma$. Moreover, the magnitude of the normal acceleration $\alpha_z$ of the DLCS was less than that of the SLCS.

The simulation program has been performed with several release points. From the results, it can be seen that the designed guidance laws were effective for the deviation of

   

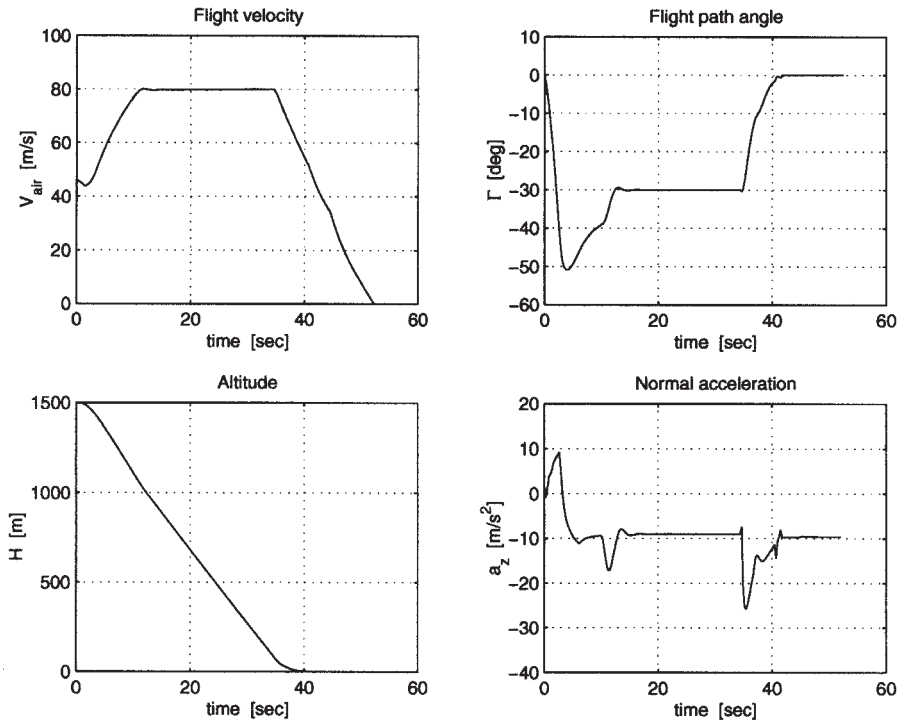


**Fig. 13** Time responses of controlled variables from release to landing by the DLCS

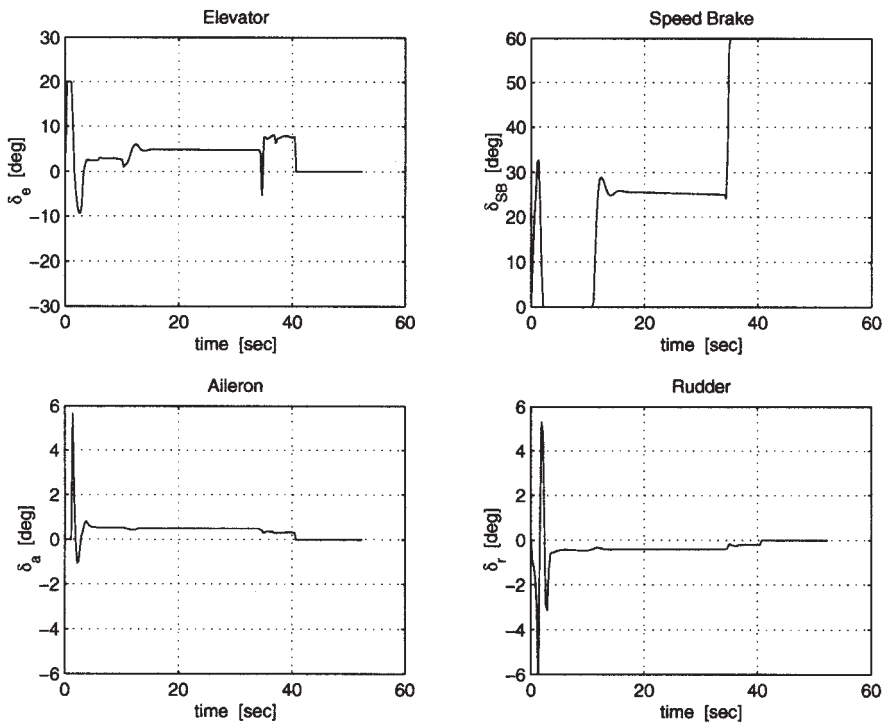


**Fig. 14** Time responses of control surfaces by the DLCS

the release point $|\Delta x_e| \leqslant 1000$ m and $|\Delta y_e \leqslant 600$ m. Thus, the DLCS was useful as a method to improve the tracking performance under the deviation of the release point from the nominal point.

## 7 CONCLUSION

This paper has presented a flight control design of an Automatic Landing FLight EXperiment (ALFLEX) re-

entry vehicle using a double-loop control system (DLCS) with the fuzzy gain-scheduling (FGS) state feedback technique. The inner-loop control law was designed by the FGS state feedback technique to guarantee the stability over the entire operating range of the ALFLEX vehicle, while the outer-loop control law was designed to improve the tracking property. Futhermore, guidance laws for the longitudinal and the lateral directions were included in the control system to navigate the ALFLEX vehicle to the reference trajectory even if the release point deviates from the nominal point. The designed DLCS showed satisfactory performance in the numerical simulation of the ALFLEX.

Since the flight condition of the ALFLEX is always not constant, there are several uncertainties in the control system. For practical implementation, the stability and performance robustness against the uncertainties should be verified through more exact simulations and test flights. This is a future subject to research.

## REFERENCES


1 **Davis, N. W.** NASDA pins its hopes on HOPE. *Aerospace America*, August 1991, 32–35.
2 **Miyazawa, Y., Ishikawa, K.** and **Fuji, K.** Guidance and control law for automatic landing flight experiment of reentry space vehicle. In Guidance, Navigation and Control Conference, Monterey, California, 1993, AIAA paper 93-3818, pp. 1057–1066.
3 NAL/NASDA ALFLEX Group. Flight simulation model for automatic landing flight experiment (Part I: free flight and ground run basic model). Technical Report of the National Aerospace Laboratory, 1994.
4 **Yanagihara M.** and **Shigemi, M.** Estimating aerodynamic characteristics of the ALFLEX vehicle using flight test data. In AFM Conference, New Orleans, Louisiana, 1997, AIAA paper 97-3485-CP, pp. 33–41.
5 **Sunazawa, S.** and **Ohta, H.** Nonlinear flight control for a reentry vehicle using inverse dynamics transformation. *J. Japan Soc. Aeronaut. Space Sci.*, 1997, **45**, 52–61.
6 **Miyajima, K.** and **Kuze, C.** Application of the neural network system to the longitudinal control system of the ALFLEX. In Proceedings of the ALFLEX/HOPE Symposium, 1996, pp. 115–118.
7 **Fujimori, A., Wu, Z.-Y., Nikiforuk, P. N.** and **Gupta, M. M.** A design of a flight control system using fuzzy gain-scheduling. In GNC Conference, New Orleans, Louisiana, 1997, AIAA paper 97-3760-CP, pp. 1647–1653.
8 **McCormick, B. W.** *Aerodynamics, Aeronautics, and Flight Mechanics*, 1979 (John Wiley, New York).
9 **Boyd, S., Ghaoui, L. E., Feron, E.** and **Balakrishnan, V.** *Linear Matrix Inequalities in System and Control Theory*, SIAM Studies in Applied Mathematics, Vol. 15, 1994 (SIAM, Philadelphia, Pennsylvania).
10 **Gahinet, P., Nemirovski, A., Laub, A. J.** and **Chilali, M.** *LMI Control Toolbox*, 1995 (The MathWorks Inc., Natick, Massachusetts).


## APPENDIX

### Proof of Theorem 1

This appendix shows the proof of Theorem 1. First, the Schur complement associated with positive definite matrices [**9**] is shown in the following Lemma.

*Lemma 1 (Schur complement)*

Let $P$ be a positive definite matrix defined as

$$P \triangleq \begin{bmatrix} P_{11} & P_{12} \\ P_{12}^{\mathrm{T}} & P_{22} \end{bmatrix} \tag{40}$$

The following statements are equivalent:

(a) $P > 0$

(b) $P_{11} > 0$ and $P_{22} > P_{12}^{\mathrm{T}} P_{11}^{-1} P_{12}$

(c) $P_{22} > 0$ and $P_{11} > P_{12} P_{22}^{-1} P_{12}^{\mathrm{T}}$

*Proof of Theorem 1.* Substituting equation (18) without the external signals into equation (19) gives

$$\begin{aligned} \frac{\mathrm{d}V}{\mathrm{d}t} &= \sum_{i=1}^{r} \sum_{j=1}^{r} \alpha_i \alpha_j x^{\mathrm{T}} (\mathbf{X}^{-1}(\mathbf{A}_i - \mathbf{B}_i F_j) \\ &\quad + (\mathbf{A}_i - \mathbf{B}_i F_j)^{\mathrm{T}} \mathbf{X}^{-1}) x \\ &< -x^{\mathrm{T}} \left( \mathbf{Q} + \sum_{i=1}^{r} \sum_{j=1}^{r} \alpha_i \alpha_j \delta_{i,j} F_i^{\mathrm{T}} \mathbf{R}_i F_i \right) x \end{aligned} \tag{41}$$

A sufficient condition of equation (41) is to satisfy the following matrix inequalities:

$$\begin{aligned} &(\mathbf{A}_i - \mathbf{B}_i F_i)\mathbf{X} + \mathbf{X}(\mathbf{A}_i - \mathbf{B}_i F_i)^{\mathrm{T}} + \mathbf{X}(\mathbf{Q} + F_i^{\mathrm{T}} \mathbf{R}_i F_i)\mathbf{X} \\ &\quad < 0 \qquad (i = 1, \ldots, r) \end{aligned} \tag{42}$$

$$\begin{aligned} &(\mathbf{A}_i + \mathbf{A}_j - \mathbf{B}_i F_j - \mathbf{B}_j F_i)\mathbf{X} \\ &\quad + \mathbf{X}(\mathbf{A}_i + \mathbf{A}_j - \mathbf{B}_i F_j - \mathbf{B}_j F_i)^{\mathrm{T}} + 2\mathbf{X}\mathbf{Q}\mathbf{X} < 0 \\ &\qquad\qquad (i = 1, \ldots, r,\ j = i + 1, \ldots, r) \end{aligned} \tag{43}$$

Defining the following variable

$$\mathbf{M}_i \triangleq F_i \mathbf{X} \tag{44}$$

and using Lemma 1, equations (42) and (43) are transformed into equations (21) and (22) where $\mathbf{Q} = \mathbf{L}^{\mathrm{T}}\mathbf{L}$. Equation (23) is obviously from the definition of $\mathbf{M}_i$ [equation (44)].